The distribution of Čerenkov Light and its effect on the separation of different classes of event by pattern recognition

M.G.Bowler, X.Chen, N.A.Jelley and M.Thorman
Nuclear and Astrophysics Laboratory, Keble Road, Oxford, OX1 3RH

November 28, 1996

Abstract

The difference in the Čerenkov light distribution as calculated by the SNOMAN code and by C.Jillings and T.Radcliffe [4] using the exact DEDRICK formalism is effectively a small difference in the width of the Čerenkov cone. This is modelled and found to have negligible effect on the ability to separate either ^{208}Tl from ^{214}Bi events or neutral from charged current events by pattern recognition. It is the difference in patterns arising from single electron and multiple electron events that is the distinguishing feature, and this is essentially unaffected by a slightly broadened Čerenkov cone. The work of C.Jillings and T.Radcliffe [4] therefore provides an elegant verification of SNOMAN's Čerenkov generation.

1 Introduction

The calculation of the distribution of Čerenkov light depends on accurately describing the electron trajectory and then evaluating the Čerenkov light emission from that trajectory. The SNOMAN code uses the EGS4 routine [1] to calculate the trajectory and this invokes the Moliere approximation to sample the direction of the electron at points along its track. It interpolates between points with part of the arc of a circle and emits Čerenkov photons along each arc at an angle appropriate to the electron's velocity. While the EGS4 implementation of the Moliere approximation, which includes both the effects of single and multiple scattering, has been validated through comparison with the Gouldsmit-Sanderson treatment of electron scattering [2], there are certain approximations in the treatment of the Čerenkov light distribution:

i) While each arc is the most probable trajectory between points on the electron's track, there will be paths that deviate from this arc and these will broaden the distribution to some extent;

ii) For a particular electron velocity, the angle of emission is not exact as there is an effective width to the Čerenkov cone of a few degrees, which is when the rms multiple scattering angle equals the diffractive width arising through the finite length of track [3];

iii) Any interference between the light emitted between arcs along the track is ignored.

To quantify this insensitivity a version of SNOMAN has been compiled in which the Čerenkov photons are emitted at an angle randomly selected between the limits given by $\theta_c \pm \delta\theta_c$, where θ_c is the Čerenkov angle. The fraction δ was set to zero or 0.2, the latter corresponding to angles between 34 and 49 degrees for electrons with energies greater than 2.75 MeV. Figure 13 shows the effect of changing $\delta = 0.0$ to $\delta = 0.2$ on the theta angle of a sample of the emitted Čerenkov photons from a single 5 MeV electron initially travelling along the z-axis. Figure 14 gives the corresponding difference in $\cos\theta_{ij}$, which is of the same kind and magnitude (as measured by the rms deviation) as seen between SNOMAN and DEDRICK for the 5 MeV track shown in figure 10. The effect of altering δ from 0.0 to 0.2 only changes the mean value of $\cos\theta_{ij}$ from 0.470 to 0.459 and such a difference has negligible effect on the ability to separate classes of events, as the following examples demonstrate.

3 Pattern recognition

The basic idea in the pattern recognition technique used to distinguish between the [208]Tl and [214]Bi decay events [7, 8, 9] is that above 30 Nhits (the number of PMTs hit), the [214]Bi decay events are mostly single electron ones while the [208]Tl decay events are always one 2.6145 Mev gamma + an electron + one or more lower energy gammas, with the consequence that the [208]Tl decay event is more isotropic than the [214]Bi decay event. In order for events arising from beta-gamma decays in the PMT's to be insignificant, only [208]Tl and [214]Bi decays within a 4 metre radius in the D_2O are considered. In distinguishing neutral and charged current (nc and cc) events in the whole volume of the D_2O, above an Nhits threshold of 60 which is above the background caused by natural radioactivity, it is the nc events that are more isotropic than the cc events, as neutron capture by ^{35}Cl gives rise to a significant number of multiple electron events.

To evaluate the effect on pattern recognition of a broadened Čerenkov cone, [208]Tl, [214]Bi, nc, and cc data were generated separately with $\delta = 0.0$ and $\delta = 0.2$. The [208]Tl and [214]Bi events with $\delta = 0.2$ were summed together, as were the nc and cc events with $\delta = 0.2$, to simulate actual data and the resulting distributions of the mean values of $\cos\theta_{ij}$ (where θ_{ij} is the angle between PMT hits) were then fitted using the distributions of the mean values of $\cos\theta_{ij}$ obtained with $\delta = 0.0$ as probability distribution functions (pdfs). The individual cc and nc plots of the mean values of $\cos\theta_{ij}$ for $\delta = 0.0$ and $\delta = 0.2$ are shown in figures 15 and 16, where it can be seen that the differences are insignificant. Figure 17 shows the $\delta = 0.2$ data and the $\delta = 0.0$ pdfs; the result of fitting the pdfs is excellent and the fitted numbers of events are: cc = 3556$\pm$161 and nc = 2445$\pm$154, for input values of 3500 and 2500, respectively.

The corresponding figures for the [208]Tl and [214]Bi data are shown in figures 18, 19 and 20 where the fitted number of events, for input values of [208]Tl = 2800 and [214]Bi = 1000, are: [208]Tl = 2760$\pm$143 and [214]Bi = 1039$\pm$131.
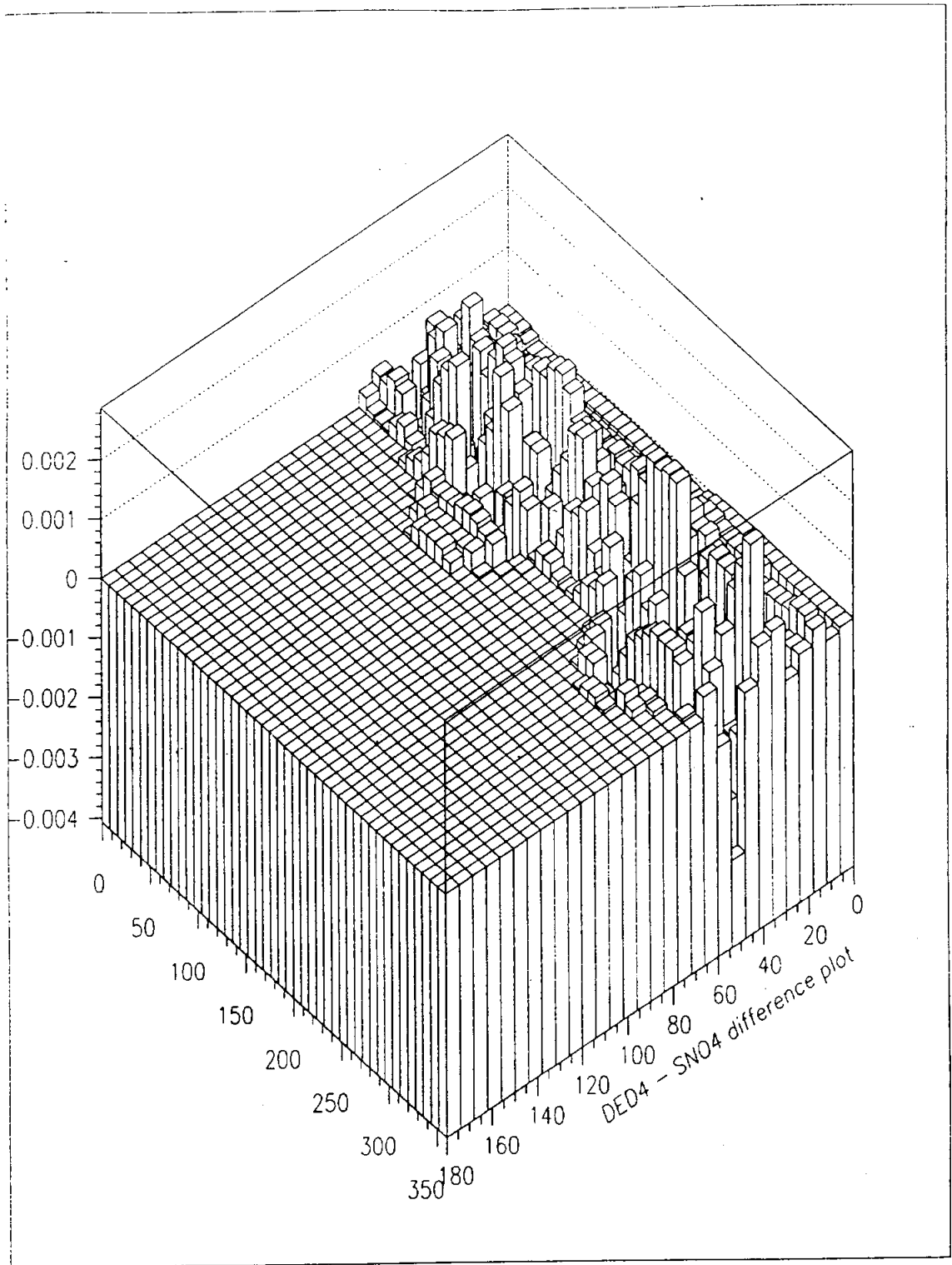
Figure 2: The DEDRICK-SNOMAN difference plot of the theta-phi distribution of Čerenkov light generated by a 5 Mev electron track aligned along the z-axis.
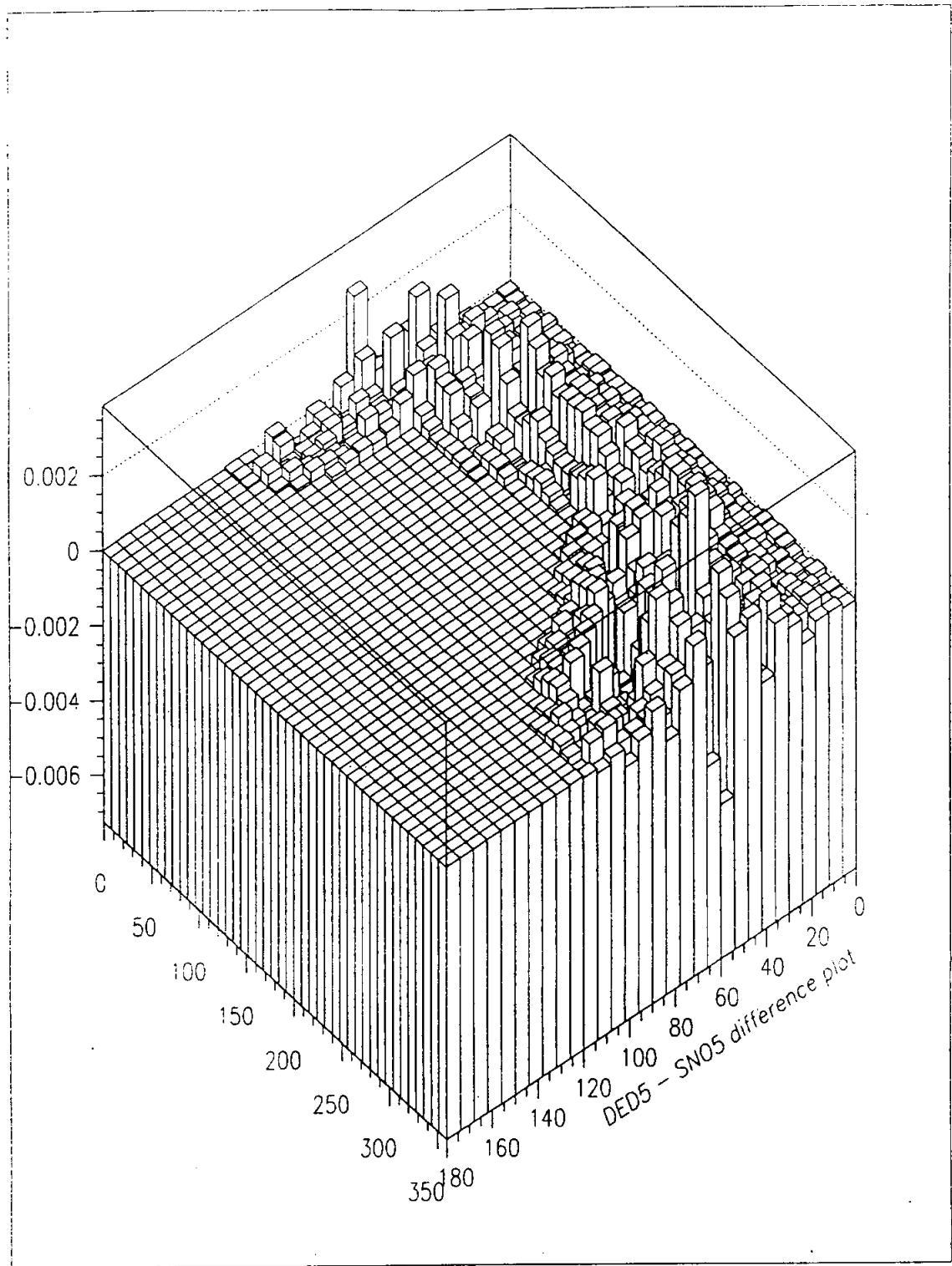
Figure 4: The DEDRICK-SNOMAN difference plot of the theta-phi distribution of Čerenkov light generated by a 4 Mev electron track aligned along the z-axis.
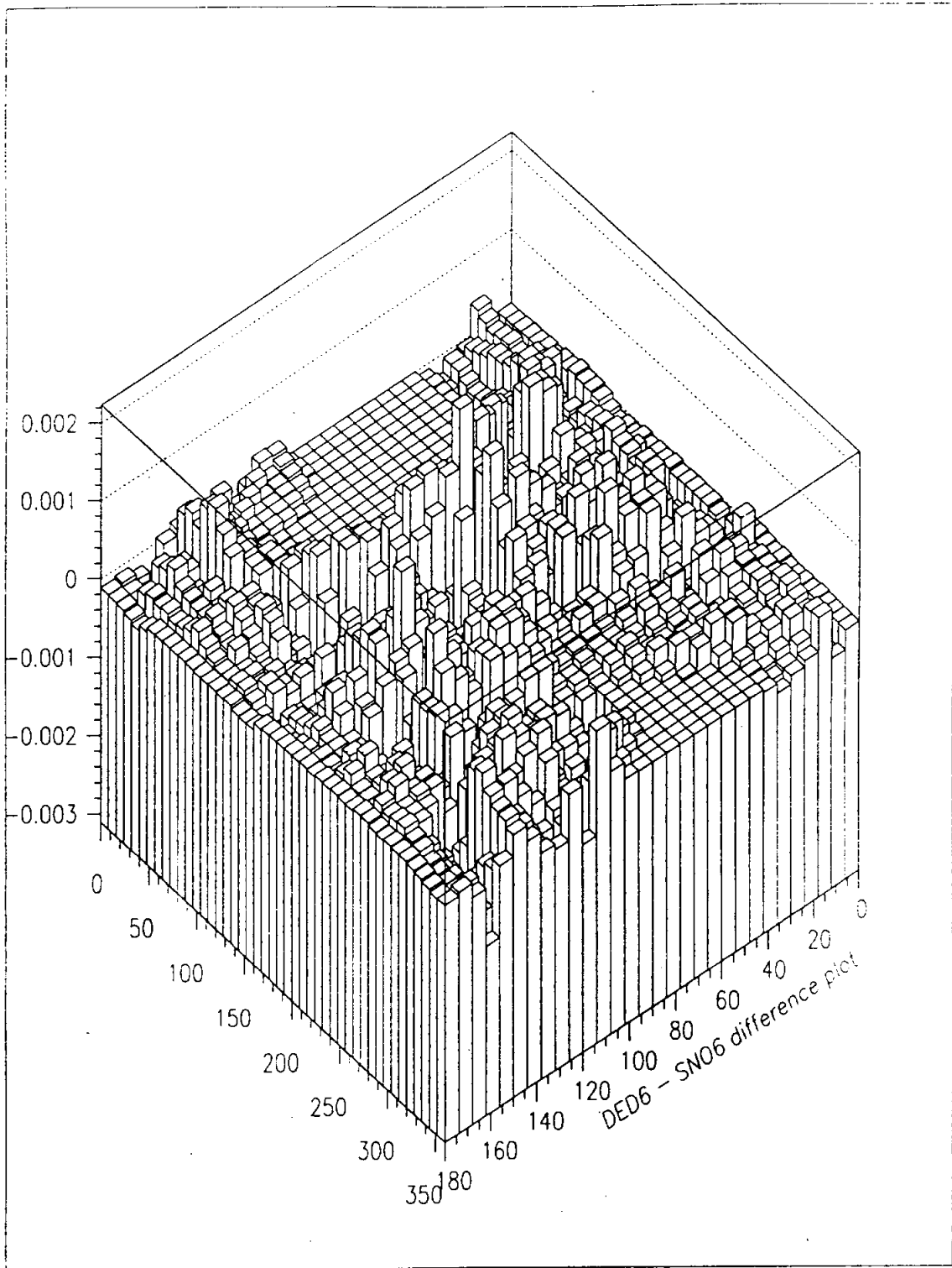
Figure 6: The DEDRICK-SNOMAN difference plot of the theta-phi distribution of Čerenkov light generated by a 1.5 Mev electron track aligned along the z-axis.
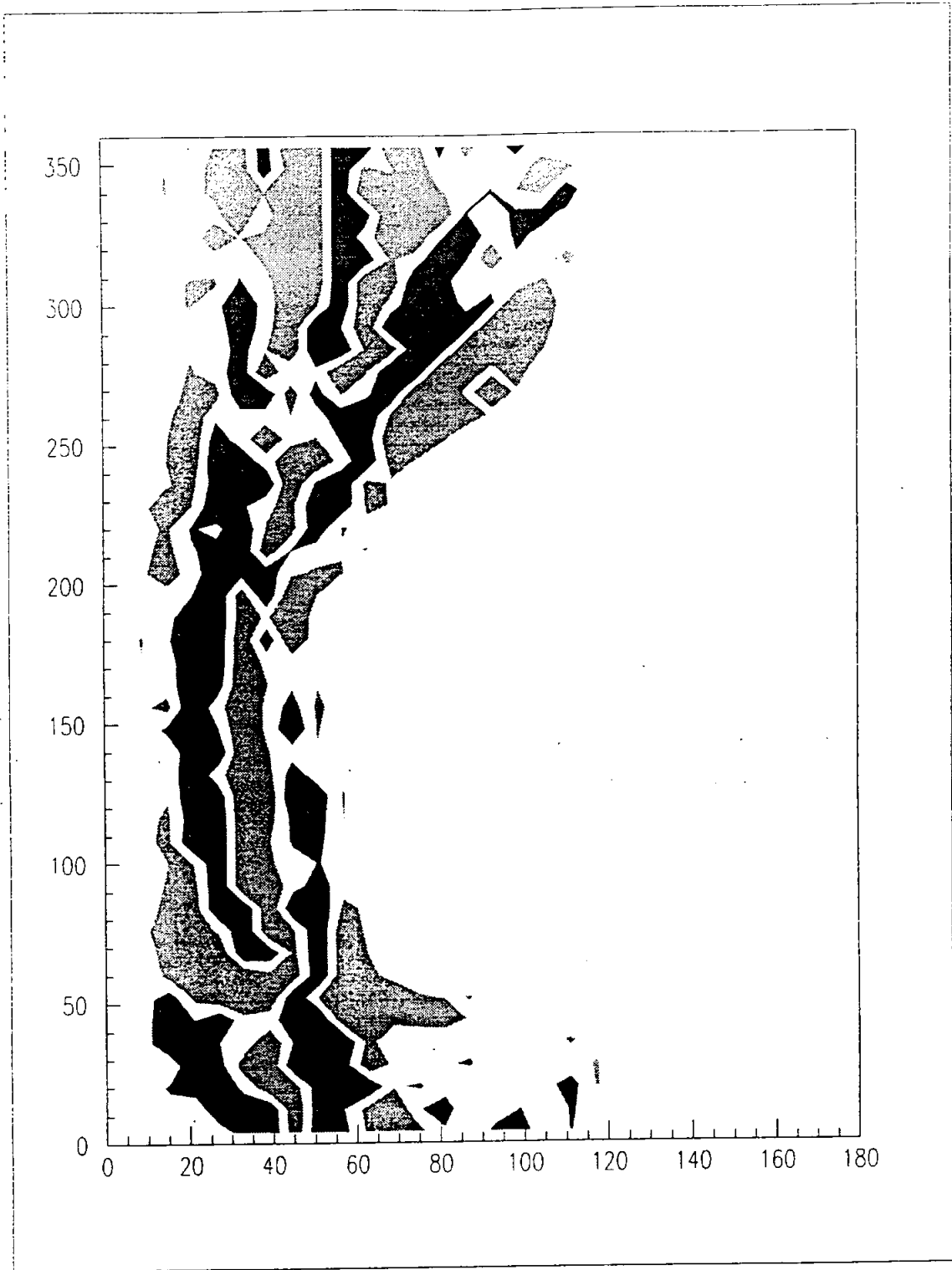
Figure 8: A contour plot of the difference SNOMAN-DEDRICK for the distribution of Čerenkov light generated by a 4 Mev electron track aligned along the z-axis. The black regions correspond to SNOMAN-DEDRICK values greater than 0.0003; the grey regions to values less than -0.0003.
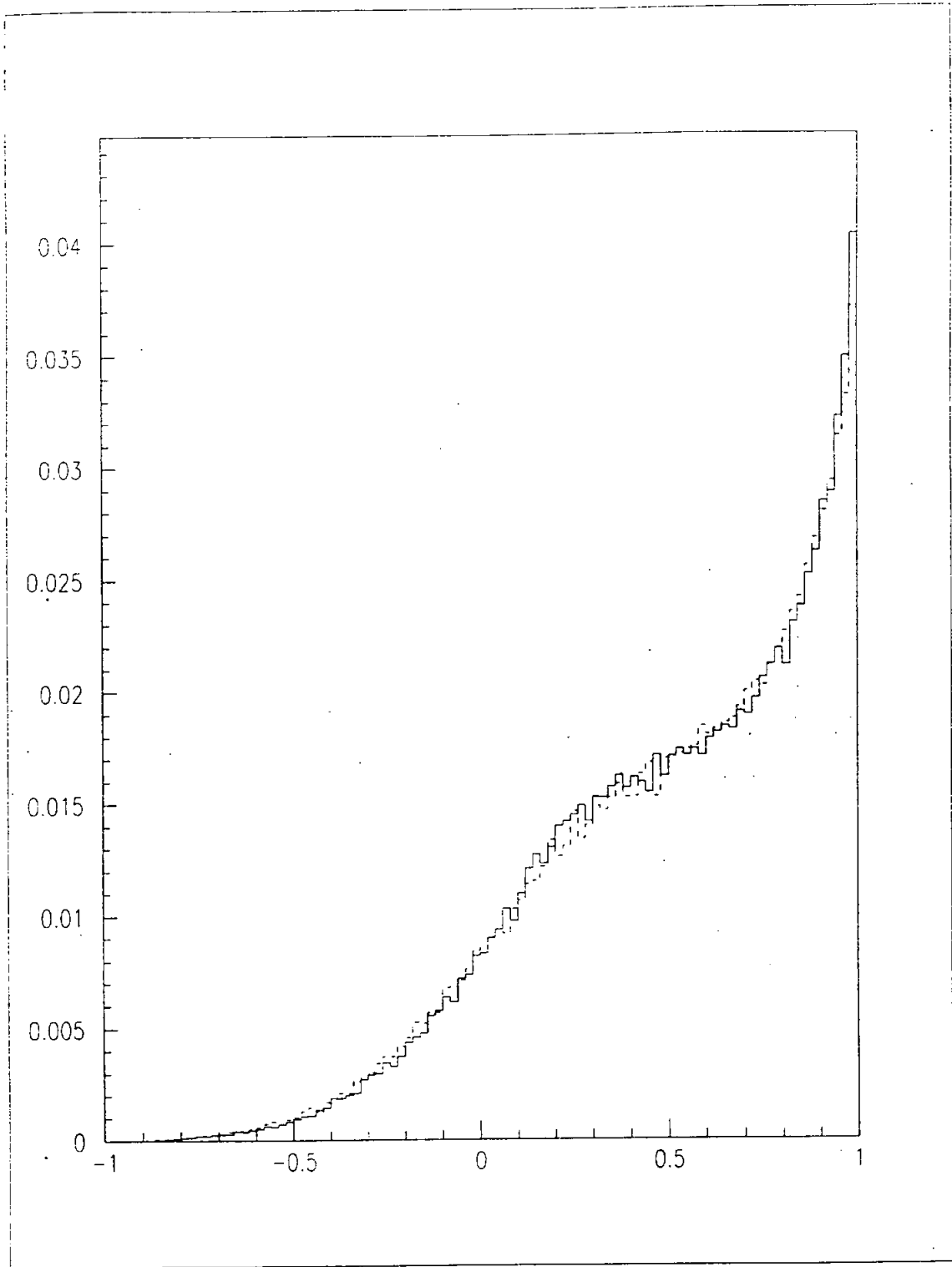
Figure 10: The distribution of $\cos\theta_{ij}$ for the SNOMAN (solid line) and DEDRICK (dashed line) distribution of Čerenkov light generated by a 5 Mev electron track aligned along the z-axis.

13
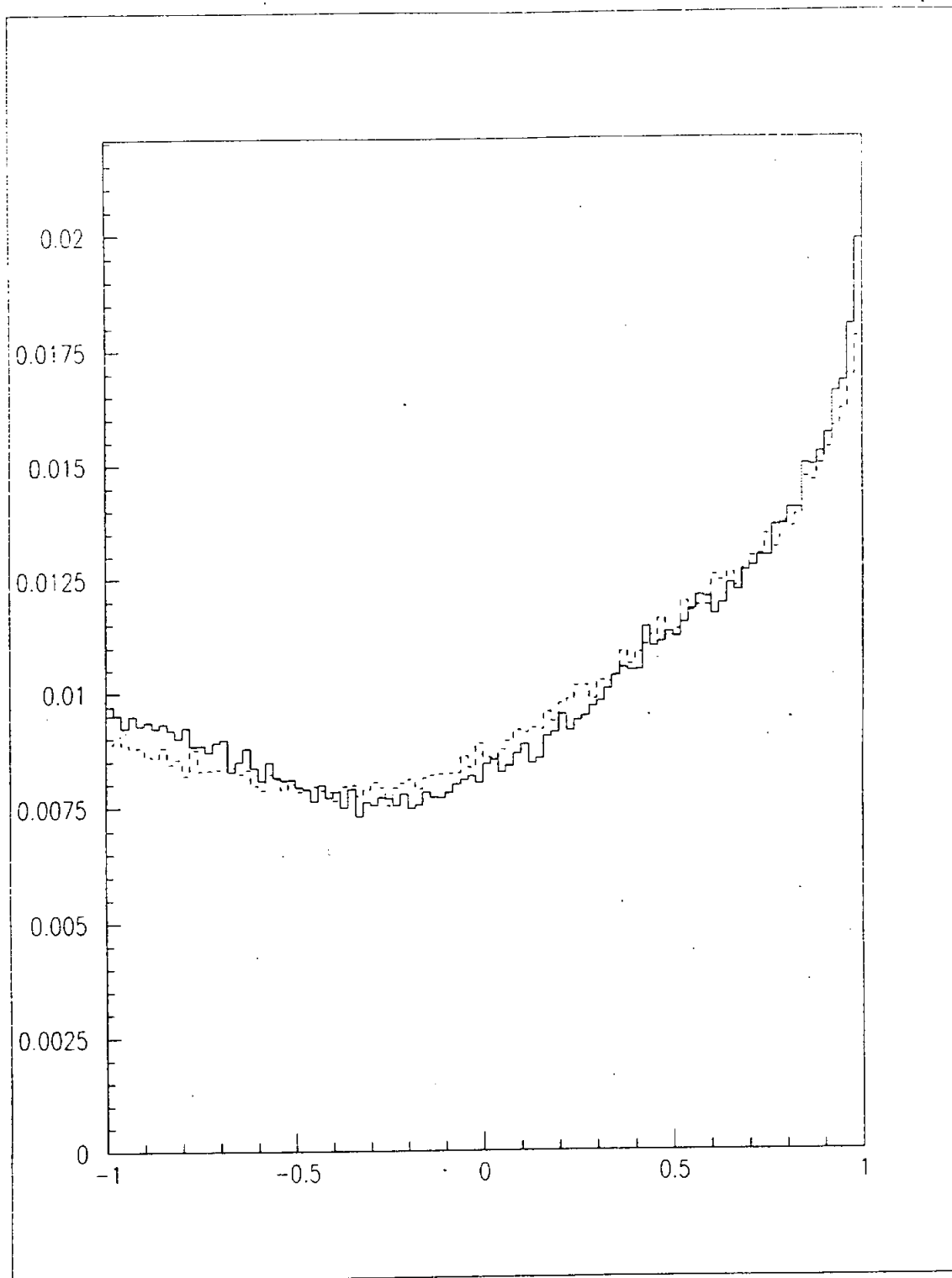
Figure 12: The distribution of $\cos\theta_{ij}$ for the SNOMAN (solid line) and DEDRICK (dashed line) distribution of Čerenkov light generated by a 1.5 Mev electron track aligned along the z-axis.
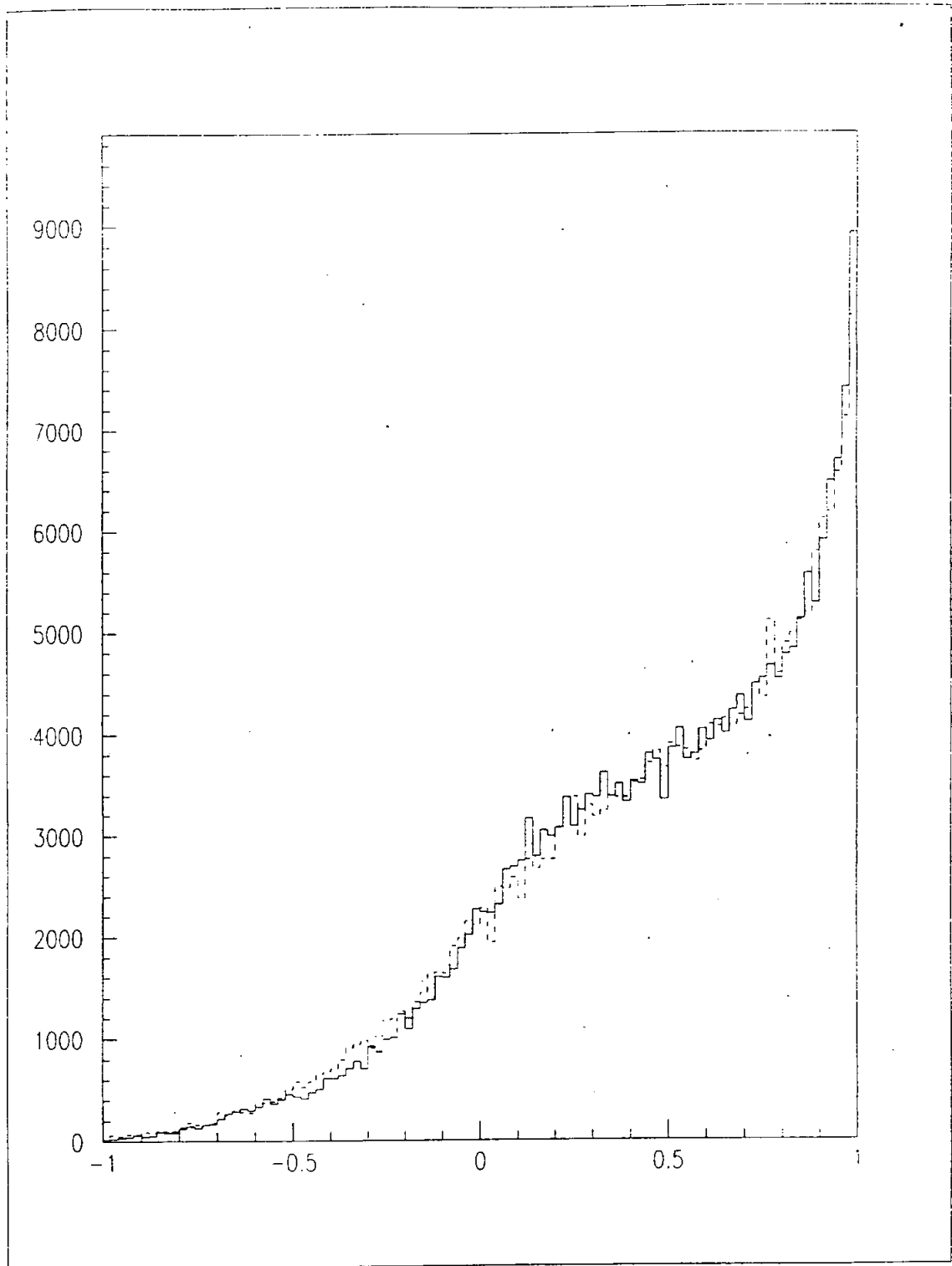
Figure 14: The distribution of $\cos\theta_{ij}$ for a single 5 MeV electron initially travelling along the z-axis for $\delta = 0.0$ (solid line) and for a broadened Čerenkov cone (dashed line) defined by $\delta = 0.2$ (see text).
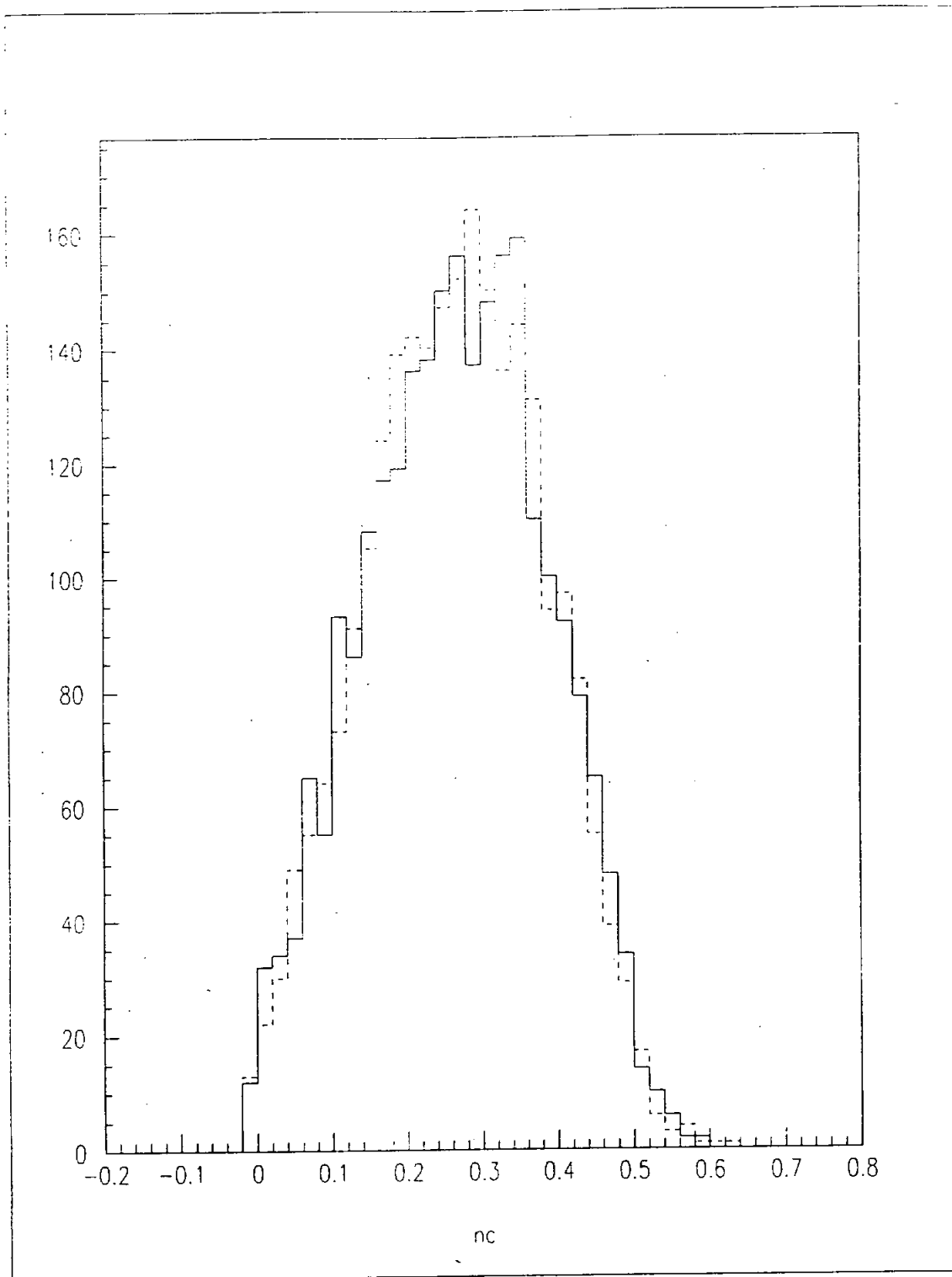
Figure 16: The distribution of the mean values of $\cos\theta_{ij}$ for neutral current data with $\delta = 0.0$ (dashed line) and $\delta = 0.2$ (solid line).
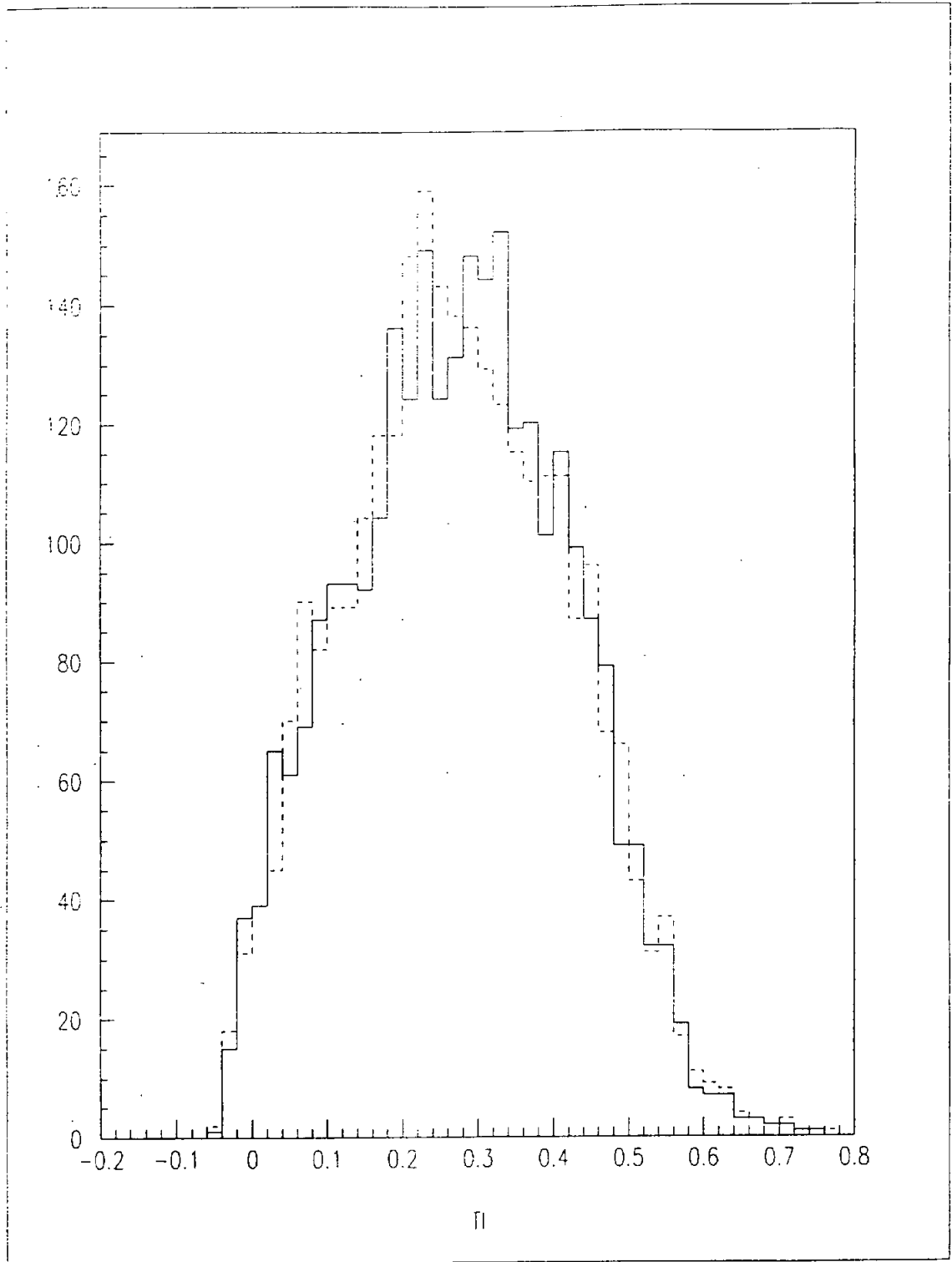
Figure 18: The distribution of the mean values of $\cos\theta_{ij}$ for thallium data with $\delta = 0.0$ (dashed line) and $\delta = 0.2$ (solid line).
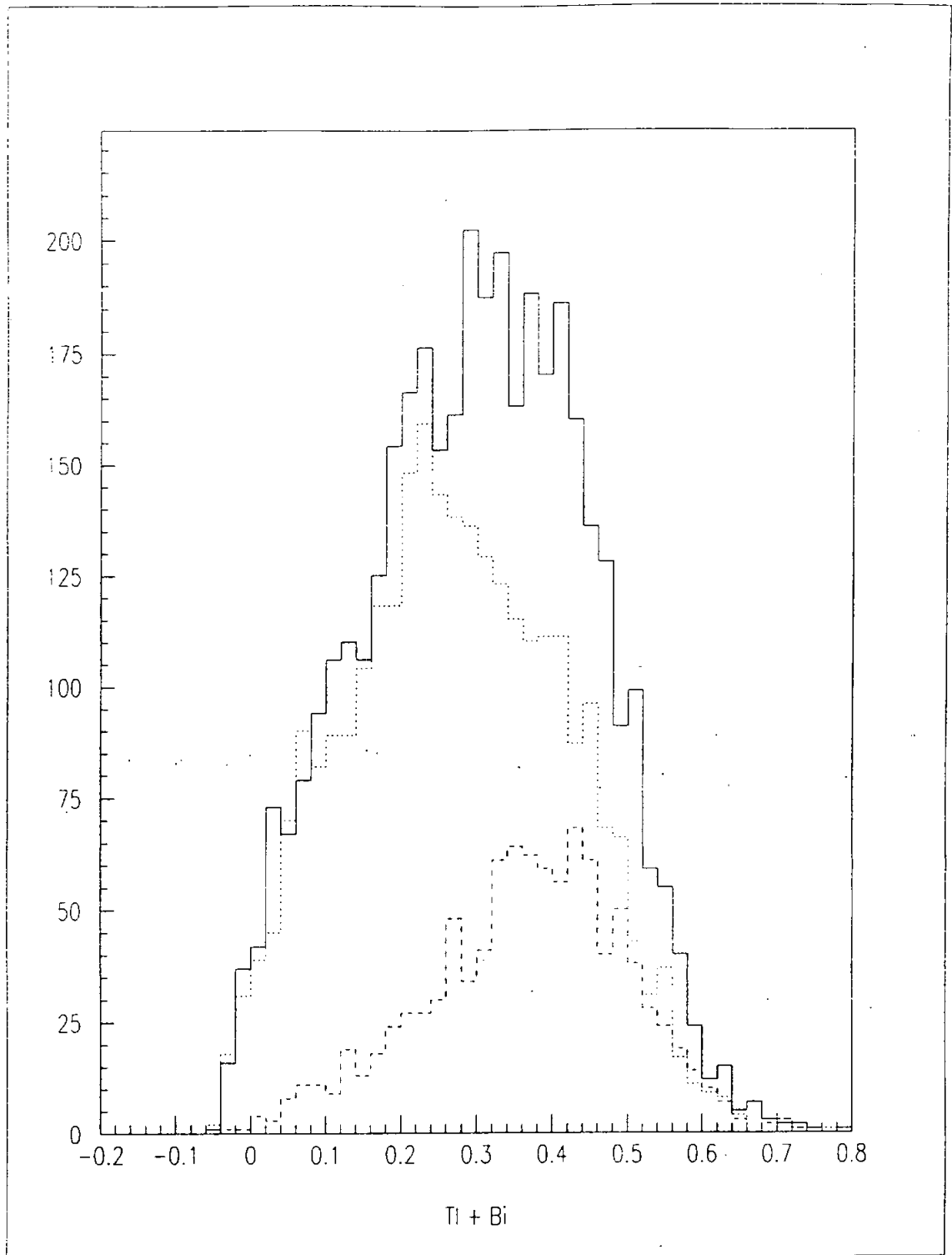
Figure 20: The distribution of the mean values of $\cos\theta_{ij}$ for the simulated thallium plus bismuth data generated with $\delta = 0.2$ (solid line) together with the $\delta = 0.0$ thallium (dotted line) and bismuth (dashed line) pdfs.